RSC Advances

ROYAL SOCIETY OF CHEMISTRY

www.rsc.org/advances

The Role of F-dopants in Adsorption of Gases on Anatase TiO_2 (001) Surface: A First-Principles Study

Huazhong Liu [a,b,c], K.M. Liew [a,*], Chunxu Pan[b]

[a] Department of Architecture and Civil Engineering, City University of Hong Kong, Kowloon, Hong Kong

[b] School of Physics and Technology and Key Laboratory of Artificial Micro- and Nano-structures of Ministry of Education, Wuhan University, Wuhan 430072, PR China

[c] Department of Basic Sciences, PLA Military Economics Academy, Wuhan 430035, PR China

*Corresponding author. E-mail: kmliew@cityu.edu.hk.

Abstract

We performed a systematic investigation of adsorption of small gas molecules (O_2, CO, NO, NO_2 and SO_2) on pristine and fluorine doped (F-doped) anatase TiO_2 (001) surface using the density functional theory (DFT). Three kinds of F-dopants, which were achieved by substituting a surface O_{2C} atom (F_I), or a surface O_{3C} (F_{II}), or an O_{3C} atom below a surface Ti_{5C} with F atom (F_{III}), were studied to investigate the effects on the surface properties as well as the adsorption of molecules. The influence of F-dopants on the adsorption energy, charge transfer and magnetic moment of the most stable adsorption configurations of these molecules on the surfaces are thoroughly discussed. Three types of F-dopants were found to have a significant promotion on the adsorption of O_2, NO and NO_2. However, the promotive effect of F_I and F_{II} dopants was not found upon the adsorption of CO and SO_2. Only F_{III} dopant was found to have promotive effect on the two molecules. The mechanisms of interactions between molecules and surfaces are examined by analyzing their electronic structure and charge transfer. The results show that Ti^{3+} induced by F-dopants plays an important role in enhancing interaction between gas molecules and TiO_2 surfaces.

1 Introduction

Titanium dioxide (TiO_2), as a photo-catalyst with excellent optical, electrical, and thermal properties, has received increasing attention. It has been extensively investigated for many applications such as gas sensors, waste water treatment and air purification.[1] Large volumes of industrial waste (toxic) gases are discharged into the atmosphere everyday. Application of TiO_2 surface properties for reduction of toxic gases has been examined theoretically and experimentally. The degradation of toxic gaseous compounds is particularly important because they represent an important type of environmental pollutants. In order to develop a new catalyst for selective catalytic reduction of toxic gases by using visible light, investigations of adsorption abilities of small molecules provide very useful information for prediction of reaction in photo-catalytic applications of TiO_2 surfaces. However, a major limitation in its practical application is the wide band gap (3.2 eV for anatase), meaning that it can only absorb ultraviolet (UV) radiation with wavelength of less than 387nm, which is less than 5% of the solar irradiance on earth surface, to excite electrons from valence band (VB) to conduction band (CB).[2] This means that a large portion of solar energy in the form of visible light is wasted in photo-catalytic applications of anatase. Therefore, it is necessary to develop a new titania-based photo-catalyst having the ability for a wide absorption scope of visible light.

Much work has been done to improve the optical response of TiO_2 under visible light excitation, for instance, by doping of transition metal ions to titania.[3] However, metal ions doped materials suffer thermal instability; an increase of

carrier-recombination centers, or the requirement of an expensive ion-implantation facility.[4] Another effective approach for extending the spectral response of TiO_2 to visible light can be achieved by doping with non-metallic elements.[4] It has been proven that absorption edge of TiO_2 to visible light region can be extended by doping with various elements such as nitrogen,[4-5] sulphur,[6] carbon,[1e] boron[7] and fluorine.[8] Asahi et al.[4] reported that the photo-catalytic activity and hydrophilicity of TiO_2 can be enhanced by nitrogen doping into substitute sites of TiO_2. Park et al.[1e] found that carbon-doped TiO_2 ($TiO_{2-x}C_x$) nanotube arrays show much higher photocurrent densities and more efficient water splitting under visible-light illumination (> 420 nm) than pristine TiO_2 nanotube arrays. Ohno et al.[6] investigated S-doped TiO_2 and found it shows strong absorption of visible light and high activities for degradation of some organic molecules such as methylene blue under irradiation at wavelengths longer than 440 nm. Lu et al.[7] studied the B-doped TiO_2 and found that under both UV and 400-620 nm visible light irradiation, the B-doped TiO_2 nanotube array electrode exhibits a higher photo-conversion efficiency than the non-doped one. As compared to other nonmetallic doped TiO_2, F-doped TiO_2 is receiving more attention not only because of its higher potential for enhancing photo-catalytic activity in visible region,[8a, 9] but also its ability to improve the stability of the active facet of TiO_2,[10] which plays the most important role in photo-catalytic applications. The anatase (001) surface, which was reported to be the most reactive facet of TiO_2 crystal and chemically more reactive than the (101) surface, may significantly affect the surface properties of anatase TiO_2 and play a key role in activities of anatase nanoparticles.[11]

Previous researchers have demonstrated that average surface energies of anatase TiO_2 are of the order of 0.90 J/m^2 for (001) surface, > 0.53 J/m^2 for (100) surface and > 0.44 J/m^2 for (101) surface.[10b, 12] The high surface energy of pristine (001) surface implies that it has high chemical activity but low stability. This would limit its technological applications. Both experimental and theoretical studies indicate that fluorine ions can markedly reduce surface energy of the (001) surface to a level lower than that of (101) surfaces through doping.[10] Moreover, crystallinity of TiO_2 can be improved by F-doping. F ions can prevent grain growth and inhibit transformation of anatase to rutile phase.[13] These fruitful investigations show bright prospects for developing the highly reactive dominant (001) facets with high crystallinity in photo-catalytic applications.

Furthermore, the mechanism of the role that F ions play in F-doped TiO_2 surfaces has also been widely explored. Despite the increasing interest and important role of F-doping in photo-catalytic application, the role of F-dopant in enhancing photo-catalytic activity seems vague as conflicting views are found in extant literature.[14] Li et al.[15] ascribed the high visible-light photo-catalytic activities of F-doped TiO_2 to the existence of oxygen vacancies in it. Yu et al.[8a] demonstrated that F-doped TiO_2 is effective for enhancing photo-catalytic activity since F-doping converts Ti^{4+} into Ti^{3+} by charge compensation and the existence of Ti^{3+} can reduce the electron-hole recombination rate. Seibel et al.[16] attributed the enhanced performance to the band gap narrowing resulting from the formation of Ti^{3+} defects induced by impurities such as F-dopant. Czoska et al.[17] claimed their F-doped samples

did not show absorption in the visible region and did not react with adsorbed O_2 to form superoxide anions. However, they found the F-dopant indeed induces the formation of states of bulk Ti^{3+} species below the conduction band. By using DFT+U method, Di Valentin et al.[14] investigated properties of at least four different types of Ti^{3+} centers, which have a key role in electron transport in n-type doped titania, and found that strongly localized solutions where an excess electron is on a single Ti^{3+} ion are very close in energy to and sometimes partly degenerate with highly delocalized solutions where the extra charge is distributed over several Ti ions. This provides important information for the conductivity mechanism in n-type doped titania. Nevertheless, the various conclusions show understanding of the interaction mechanism of Ti^{3+} induced by F-dopant in n-type doped titania which appears to be an appealing challenge. So far, little theoretical work has reported how F-doped TiO_2 surface, especially Ti^{3+} induced reactive (001) surface, affects gas molecules adsorbed on it. The role of Ti^{3+} induced by F-dopant in adsorption of gases is also unclear. Thus, it is reasonable to believe the knowledge of interaction between the gases and F-doped TiO_2 surface will result in a new understanding of the role of F-dopants in n-types doped titania.

As discussed in a review,[18] many works have reported that it is difficult to provide a satisfactory description of properties of defects (for example, Ti^{3+} in TiO_2) in insulators by using the standard DFT method since non-local factors in the exchange-correlation (XC) functional are ignored. An alternative methodology used to eliminate or reduce this failure is the so-called DFT+U method.[19] This method

introduces a Hubbard-U term in the functional, representing an on-site Coulomb repulsion among selected orbitals, to better describe the electron correlation effects of d-orbitals. This acts to remove the self-interaction error and the consequent tendency to delocalize unpaired electrons and reduce the Coulomb repulsion in the standard DFT, which fails to correctly describe the localized states in the system, such as the F doped TiO_2. This method corrects some of the inadequacies connected to the standard DFT treatment of localized states, but is dependent upon a tunable parameter of U value.[20] The determination of an appropriate U parameter value for TiO_2 has always been discussed,[20-21] nevertheless, we cannot expect to find a universal U value to fit all physical properties of TiO_2 perfectly. The U value is usually considered as an empirical term which varies until convergence with the experimental results. The values of U can be determined through the method so as to account for the experimental results of physical properties such as structural parameters, magnetic moments, band gaps, redox potentials, or reaction enthalpies.[21b] On the whole, previous DFT + U works[22] indicate that a value of U = 10 eV for rutile TiO_2 and U=8.5 eV for anatase TiO_2 to match the experimental band gap and U value in the range of 2~6 eV is suitable to describe the properties of TiO_2 such as structural parameters and electronic structure.[20, 23] Moreover, the localized electron in Ti^{3+} species is successfully described by using a U value of 3~4 eV. [14, 23c, 24]

The present study focuses on studying adsorption of some common gas molecules (O_2, CO, NO, NO_2, SO_2) on pristine and F-doped anatase TiO_2 (001) surfaces using DFT calculations, which include spin polarization calculations in

open-shell systems, by employing the GGA+U method. Based on this method, effects of three kinds of F-dopants adjacent to Ti atom at the adsorption site have been thoroughly investigated. Adsorption abilities, in terms of adsorption energy and charge transfer, charge difference and projected density of states (PDOS) of all gases are analyzed to examine their behaviors on these surfaces. The purpose of this work is to provide improved insights into the fundamental understanding of the nature of interactions between adsorbate and F-dopants in n-type doped titania for a better design of the titania-based photo-catalyst and sensors.

2 Computational Details

We performed periodic spin-polarized density functional theory (DFT) calculations using GGA+U method[25] with Perdew and Wang (PW91) functional,[26] as implemented in the Quantum Espresso code.[27] The ultrasoft pseudopotentials[28] method was used in this work, where the 3s, 3p, 4s and 3d shells of Ti atom, the 2s, 2p shells of O, F, N and C atoms and 3s, 3p shells of S atom were treated as valence shells. The cutoffs for smooth part of the electronic wave-function and the augmented electron density were set to 30 and 300 Ry, respectively. The convergence threshold for self-consistency was set at 1.0×10^{-8} Ha. The ground-state geometries of bulk and surfaces were obtained by minimizing the forces on each atom until the residual forces were below 1.0×10^{-3} Ha/Å. This force convergence criterion is close to the value adopted in previous studies.[11e, 11f] We obtained the bulk lattice parameters, a=3.790Å and c=9.646Å, by using a k-point grid of (4 × 4 × 2). This result agrees

well with the previously reported experimental and theoretical results,[29] confirming the authenticity of our calculations.

In order to estimate an appropriate value of U, a series of U values ranging from 2 to 9 eV have been examined. The outcomes indicate that U=2.0 eV is sufficient to describe the localized state in band gap induced by F dopant. For obtaining the band gap with experimental value of 3.2 eV, our calculations show that a value of 8.1 eV is required, which is close to Deskins et al.[22a] However, such a large value would lead to relatively large overestimated lattice constants, which in turn may cause a structurally bad prediction. Our results show that the overestimation of lattice constants gets enlarged within the GGA+U, ranging from 2.7% for U = 4 eV to 3.8% for U = 9 eV. The lattice constant is overestimated by about 1.5% within the standard GGA in our outcomes. Thus, we consequently use, throughout this work, the lattice constants optimized for plain DFT (U=0). The effect of this choice on the obtained density of states (DOSs) is minimal. In the case of F dopant using DFT+U with U=3.8 eV, we found less than 0.02 eV difference in the position of the localized states below the CBM when using the two sets of lattice constants. We cannot expect a selected U value that will give all correct properties of TiO_2, but it is important that a U value of 3.8 eV can provide a correct description of impurity states in the band gap. As a result, we adopted the U value of 3.8 eV for describing the valence electrons of Ti atom in this work.

The pristine anatase (001) surface (denoted as PT) represented by a slab in a super-cell consisted of neutral (O-Ti-O) repeating tri-layer units (Figure 1a). The

(001) surface is terminated by five-fold coordinated Ti atoms (Ti_{5C}) and two- and three-fold coordinated O atoms (O_{2C}, O_{3C}), while the bulk consisted of three-fold coordinated O atoms (O_{3C}) and six-fold coordinated Ti atoms (Ti_{6C}). The slab was formed from a (2 × 2) super-cell (0.25 ML) with a thickness of four tri-layers (~7.8 Å thick) and a surface area of 7.58 × 7.58 $Å^2$, containing a total of 12 atomic layers and 16 TiO_2 units per super-cell. For small molecules, a surface area of (2 × 2) on anatase (001), which was proven to be large enough to avoid lateral repulsion between the adsorbed molecules in adjacent super-cells, was adopted in previous works.[11a, 30] Moreover, a slab with a thickness of four O-Ti-O tri-layers is sufficient for convergence of the (001) surface structure and energy[11b, 31] that has been used in previous studies[11f, 30a, 30c, 32] of adsorption systems involving anatase (001). Therefore, we mainly focused on adsorption behaviors of molecules in the (2 × 2) super-cell (48 atoms) with four tri-layers. The F-doped TiO_2 (001) surface (denoted as FT) was produced by replacing one lattice O atom by F atom in the super-cell surface of PT. In order to get a quantitative comparison of activities of PT and FTs, we constructed a super-cell model containing slabs with two equivalent surfaces (i.e. a crystal with inversion symmetry) to calculate the surface energy (E_{surf}) for both surfaces. The surface energy E_{surf} is defined as follows:[11b, 33-34]

$$E_{surf} = (E_{slab} - nE_{bulk}) / 2A \qquad (1)$$

where E_{slab} is the total energy of the slab, E_{bulk} is the total energy of the single TiO_2 bulk unit cell, from which the slab is created, A is the area of the slab surface, n is the number of TiO_2 unit cells contained in the slab surface and a factor 1/2 is used

because the slab has two surfaces. Note that for an F-doped system, the slab should have the same concentration of F ion with respect to bulk model from which the surface is cleaved.

To investigate the adsorbate-substrate interactions, we mainly focus on the most stable molecular adsorption configuration having the lowest total energy and the highest adsorption energy. Adsorption energy E_{ads} is defined as

$$E_{ads} = E_{molecule} + E_{substrate} - E_{molecule/substrate} \quad (2)$$

where $E_{molecule}$, $E_{substrate}$ and $E_{molecule/substrate}$ denote energies of the isolated gas molecule, bare substrate of pristine TiO_2 slab (or F-doped TiO_2 slab) and the combined molecule-substrate system, respectively.

In all slab models, as implemented in our previous work, atoms in the bottom two tri-layers of the slab were kept fixed at the optimized bulk positions and the other atoms were fully relaxed. Different k-point samplings from (1 × 1 × 1) to (3 × 3 × 1) were tested for the bare (001) slab surfaces and adsorbed systems. The (2 × 2 × 1) sampling grid was found to be accurate enough, with less than 0.01 eV difference in adsorption energy to the (3 × 3 × 1) k-point mesh. Therefore, we decided to use a (2 × 2 × 1) grid for our work involving the anatase (001) surface.

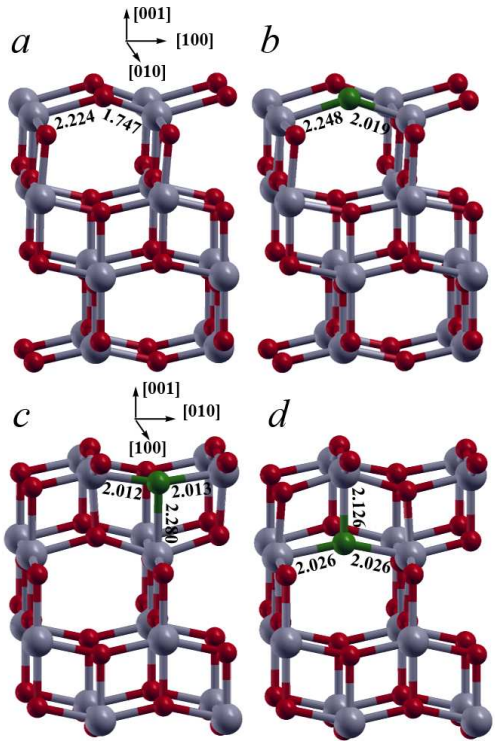

Figure 1: Optimized structures of pristine and F-doped anatase TiO_2 (001) surfaces. Side view of: (a) pristine; (b) F_I doped; (c) F_{II} doped; and (d) F_{III} doped surfaces. The Ti atoms are in gray, O atoms are in red and F atoms are in green. These notations are used throughout this paper.

3 Results and Discussion

3.1 The bare Pristine and F-doped anatase (001) surfaces

As a preliminary calculation, we first investigated the properties of pristine and F-doped bare surface. On the PT (Figure 1a), after optimization, the O_{2C} atoms are displaced outwards and the O_{3C} atoms are displaced inwards on the (001) surface (0.12 Å for O_{2C} atoms and 0.01 Å for O_{3C} atoms). The Ti_{5C} atoms on the surface are relaxed inwards by 0.05 Å. The mirror plane symmetry along [100] direction is broken: the two O_{2C}-Ti_{5C} bonds become nonequivalent, with the two optimized Ti-O

bond lengths of 1.747 Å and 2.224 Å, respectively. The asymmetric Ti-O bond structure of (001) surface obtained by the theoretical methods have been reported in the privious works.[11,12] The distance for in-plane O atom and Ti atoms ($r(Ti_{5C}\text{-}O_{3C})$) is ~1.948 Å. A surface energy of 0.92J/m^2 was obtained for the PT. These results agree with our previous results obtained by GGA method[35] and are also in close agreement with other theoretical reports.[11b, 12, 34]

For FT, we considered three kinds of F-dopants, in which F atom was substituted for a surface O_{2C} atom, or a surface O_{3C} atom, or an O_{3C} atom below a surface Ti_{5C} atom. We denote them as F_I, F_{II} and F_{III}, respectively. The corresponding surfaces are denoted as F_IT, $F_{II}T$ and $F_{III}T$, respectively. The selected doping sites are all adjacent to the surface Ti_{5C} atom, representing F-dopants of different depths. As compared to O atom in PT, F-dopants induce a larger atomic separation in the surface. For example, on F_IT (Figure 1b), the two asymmetric F-Ti_{5C} bonds, which have values of 2.019 and 2.248 Å, are larger than that on PT formed by O_{2C} and Ti_{5C}. The bond lengths of F-Ti_{6C} in $F_{II}T$ (2.280 Å, shown in Figure 1c) and F-Ti_{5C} in $F_{III}T$ (2.126 Å, see Figure 1d), are also larger than the bond lengths of 1.983 and 1.938 Å at the same location in PT. Apart from that, the lattice is only slightly distorted by F-dopants. Surface energies of F_IT, $F_{II}T$ and $F_{III}T$ are calculated to be 0.74, 0.92 and 1.04 J/m^2, respectively. This reveals that the F-dopants with different depths behave differently. The lowest surface energy of F_IT and the highest surface energy of $F_{III}T$ among the FTs demonstrate that the F-dopants in the uppermost surface and subsurface have distinctly different effects on the activity of TiO_2 surface.

The PDOS analysis (see Figure 2) shows that the Fermi level at the mid band gap for PT has changed upon inducing F-dopant. In all F-doped cases, below and close to the Fermi level, F doping induces a new localized spin state corresponding to the Ti^{3+}. This state is a consequence of introducing a fluorine substitution which leaves an extra electron in the lattice. Based on the polaron theory,[36] the excess unpaired electron is highly localized in Ti 3d shell and causes its reduction from Ti^{4+} to Ti^{3+}. This is confirmed in Figure 2, which shows the PDOS for FTs. An inspection of PDOS showed that the localized Ti^{3+} states, which correspond to an excess electron induced by F-dopants, lie at 0.8~1.1 eV below the bottom of CB. The orbitals corresponding to these spin polarized states have a distinctive shape of 3d orbital in Ti ions (Figure 2). It is noted that all Ti^{3+} produced by the three different F-dopants are located at a subsurface Ti_{6C} atom, neighbor or next neighbor to the F-dopant (Figure 2). The polarized electron located in Ti^{3+} induces a magnetic moment of $1\mu_B$ to FT. The introduction of electron donor thus makes the system an n-type semiconductor and introduces reduced states, thus changing chemical properties of the surface. The formation of lattice Ti^{3+} as a consequence of fluorine doping in TiO_2 crystal is fully supported by the theoretical calculations.[14, 17] Experimentally, a localized polaronic picture of the resulting Ti^{3+} species was reported to better fit the mechanism of hopping for electron transport in TiO_2.[14, 36] The excess electrons located in orbitals of Ti^{3+} may cause some primary influences on adsorption properties of the surfaces. For example, they may play a key role in and dictate the ensuing surface chemistry, such as providing the electronic charge required for O_2 adsorption and dissociation.[37]

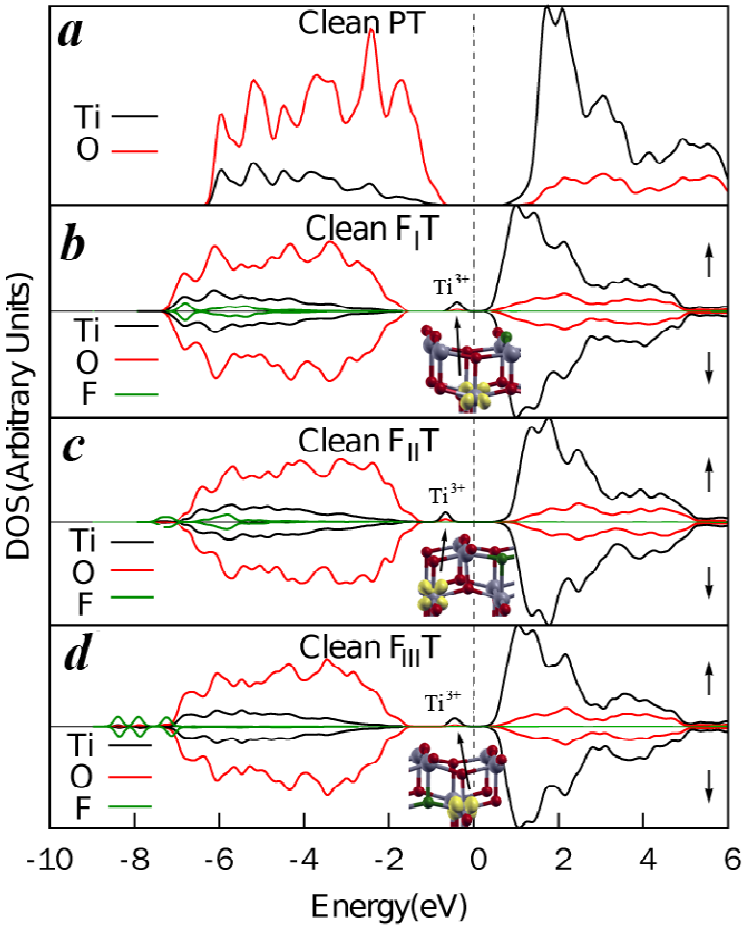

Figure 2: Projected density of states (PDOS) for pristine and F-doped surfaces. The PDOS for: (a) pristine; (b) F_I-doped; (c) F_{II}-doped; and (d) F_{III}-doped surface. Insets show where Ti^{3+} locates in the surface. The Fermi level is set to zero. The arrows in the right side of the panels denote the spin-up (↑) states and spin-down (↓) states. These notations are used throughout this paper.

3.2 Gases adsorbed on pristine and F-doped anatase (001) surface

3.2.1 O_2 adsorption

Reactive oxygen species (O_2^-) produced by O_2 adsorption on surfaces function as important intermediates in both total and selective catalytic oxidation.[38] The O_2^-

species on metal oxides can be characterized by using ESR technique through detecting the effects of electric field at the surface.[39] Anpo et al.[38b] proposed that O_2 would be adsorbed on an n-type semiconductor surface. Thus, it is meaningful to investigate the mechanism of O_2 adsorption on F-doped surfaces. We examined adsorption of O_2 on different adsorption sites and found the most stable adsorption configuration of O_2 on clean TiO_2 (001) has an adsorption energy of -0.1 eV, indicating that O_2 adsorption on clean TiO_2 (001) is endothermic and hence it is impossible to occur spontaneously in reality; this is in agreement with previous studies.[30c] After F-dopant has been introduced to the surfaces, O_2 was found adsorbed quite strongly on them with a significant charge transfer (Table 1). It was predicted in the previous report that adsorption of O_2 takes place on titania surface after the formation of Ti^{3+} through charge transfer.[40] On all FTs (F_IT, $F_{II}T$ and $F_{III}T$), the O_2 molecule can be adsorbed as the most stable configuration, via two O atoms bonding to the same Ti atom with the molecule parallel to the surface (Figure 3). Among the three kinds of F-dopants, F_{III} has the most promotive effects on O_2 adsorption. The adsorption is the strongest with adsorption energy of 1.67 eV on $F_{III}T$ (Table 1).

Importantly, during the relaxation of O_2 bonding to F-doped surface, we found that the excess electron first transfer from its original location, a subsurface Ti_{6C}, to a surface Ti_{5C} which bonds to the O_2, then to the adsorbed O_2. This may be because when O_2 approaches the surface, it deforms the local electric field near the adsorption site. Deformation of the local electric field on the surface can be detected by EPR technique.[38b, 39] Deformation of this kind makes Ti^{3+} transfer from the subsurface Ti_{6C}

atom to the surface Ti_{5C} atom where O_2 is adsorbed and then an undercoordinated surface Ti^{3+} forms. The undercoordinated (Ti_{5C}) Ti ions are believed to play a relevant role in stabilizing the extra charge at the surface and making it available for charge transfer to adsorbates.[41] After the O_2 molecule reaches its equilibrium position, the Ti^{3+} state vanishes and an unoccupied state of O_2 appears at the bottom of CB. All three O_2/FT systems have a magnetic moment of $1\mu_B$ but it is different in the cases of clean FTs in which the polarized electron is located on Ti^{3+}, the magnetic moment is induced by radical anion O_2^- (shown in inserted panel of Figure 4).

The PDOS gives the bonding mechanism of O_2 adsorption (Figure 4). The localized Ti^{3+} state at the bottom of CB, which contains an extra electron introduced by F-doping, is close to the Fermi energy and above the $2\pi^*$ orbitals of O_2, making transfer of one electron from Ti^{3+} to the $2\pi^*$ orbitals of O_2 easy. Then O_2 acts as an electron acceptor and destroys the Ti^{3+} with formation of superoxide anions. The presence of three electrons in the two $2\pi^*$ orbitals results in paramagnetism of O_2^- species and becomes the source of magnetic moment of adsorption systems. After charge transfer occurs, Ti^{3+} disappears. The states of Ti^{3+} move to about 0.6 eV above the Fermi level and the corresponding Ti 3d orbital becomes empty (Figure 4). Due to injection of electrons into anti-bonding $2\pi^*$ orbital, the adsorbed O_2 molecules have an obvious elongation in O-O bonds. As compared to the clean FTs, Fermi energies of O_2-substrate systems shift to a lower location of band gap upon the adsorption of O_2. Generally, the impurity state in the gap originating from Ti^{3+} has a distinctly promotional effect on adsorption of O_2 and makes O_2 an electron acceptor

accompanied by a significant charge transfer. As a whole, we can draw conclusions on the relationship between F-dopants and O_2. When F-dopant is induced into the surface, the excess electron transfers from F ion to Ti^{4+} and generates Ti^{3+}. After O_2 reacts with this n-type surface, the electron transfers from Ti^{3+} to the adsorbed O_2. Thus, in this process, the Ti^{3+} acts as a necessary bridge for electron transfer from surface to O_2. The electrons transfer from Ti^{3+} of the adsorbed oxygen species on the surface was believed to slow down recombination rate of the electron-hole pairs in the surface and enhance photo-catalytic activity.[8a]

Table 1: Relaxed structural parameters (bond lengths), adsorption energies (E_{ads}), charge transfer (ΔQ) and magnetic moments (M) of O_2 molecule in gas phase or adsorbed on F-doped surfaces (F_IT, $F_{II}T$ and $F_{III}T$) in the most stable configurations. The subscript 's' indicates the atom is at the surface which bonds to the molecule; otherwise, it belongs to the adsorbed molecule. This notation has the same meaning in other tables.

Gas/Substrate	O(1)-Ti_s(Å)[a]	O(2)-Ti_s(Å)[a]	O(1)-O(2)(Å)	ΔQ(|e|)[b]	M(μ_B)	E_{ads} (eV)
O_2 (gas phase)	-	-	1.232	-	2.0	-
F_IT	2.032	2.032	1.328	-0.504	1.0	0.75
$F_{II}T$	2.022	2.023	1.328	-0.517	1.0	1.42
$F_{III}T$	2.013	2.016	1.332	-0.522	1.0	1.67

[a] The labels of O atoms are shown in Figure 3.

[b] The charge transfer is obtained by Bader charge analysis. A negative value indicates the molecule gains electrons from substrate, and vice versa. This expression is also applicable to later tables.

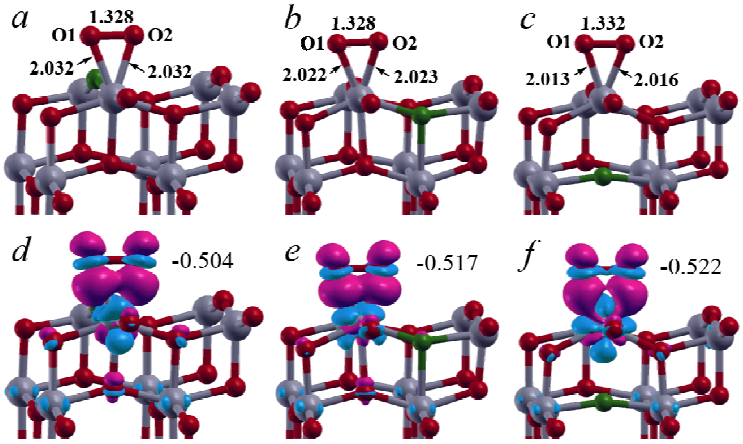

Figure 3: Optimized adsorption geometries and charge transfer of O_2 molecule on F-doped surfaces in the most stable configurations. The upper panel shows adsorption geometries of O_2 on: (a) F_I-doped; (b) F_{II}-doped; and (c) F_{III}-doped surface; the lower panel (d~f) shows the corresponding charge transfer between them. In the lower panel, purple and light blue colors represent positive (gaining electrons) and negative (losing electrons) values, respectively. The isosurface value of each case is 0.005 e/bohr^3. The decimals denote the net charge on the molecule. A negative value of charge transfer indicates that the molecule gains electrons from the surface. These notations are used throughout this paper.

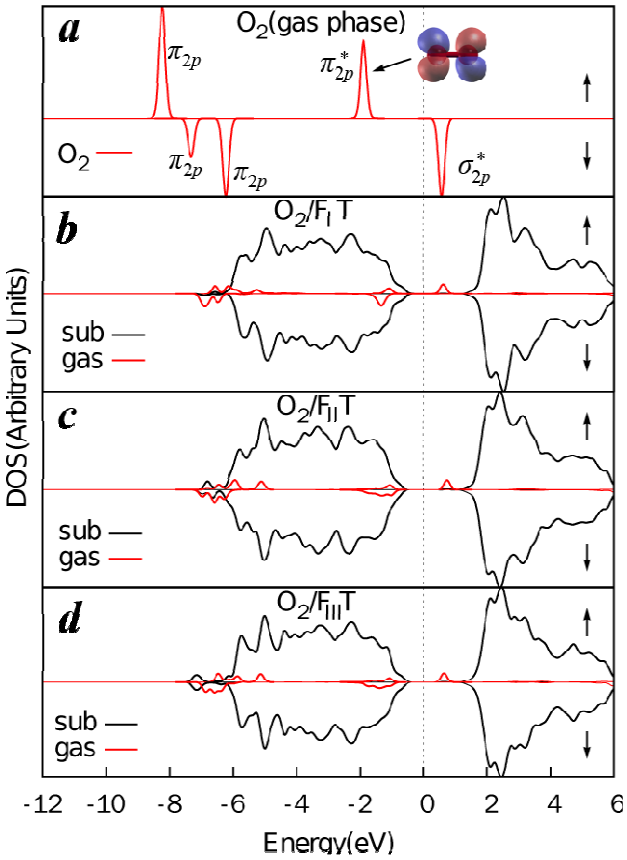

Figure 4: Total density of states (TDOS) for: (a) a gas-phase O_2 molecule and PDOS, (b) O_2 on F_IT; (c) O_2 on $F_{II}T$ and (d) O_2 on $F_{III}T$. The Fermi level is set to zero. The notation of "sub" denotes the states of substrate, and "gas" denotes the states of the adsorbed molecule (O_2). These notations are used throughout this paper.

3.2.2 CO adsorption

CO is another most common probe molecule used for studying properties of catalyst surfaces. Investigations of mechanisms of CO-substrate interaction[42] have contributed to insights into surface chemistry of some transition metal oxides catalysts, such as Al_2O_3, Ti_2O_3, V_2O_3, Cu_2O and Ag_2O. However, little work has been carried out to study the interaction of CO with F-doped TiO_2. We expect an investigation of

CO adsorption on F-doped TiO_2 to provide a deeper understanding of the influence of F-dopants upon titania-based catalyst.

Pertaining to adsorption of CO on PT and FTs, we focus discussions on the most stable configurations. The most stable adsorption of CO on PT is on the bridging site where Ti-O bond breaks and CO molecule embeds in the site between Ti_{5C} and O_{2C} atom, to form a cable-stayed bridge structure (Figure 5a). In this configuration, the C atom of CO bonds to both O atom and Ti atom and the O of CO bonds to Ti_{5C} atom. The surface is greatly distorted with the O_{2C} atom being pulled out from the surface and deviates from its original location by 1.091 Å, implying this configuration is a chemical adsorption. Experimental works have reported that upon exposure to CO, a large portion of carbon monoxide is reversibly chemisorbed on TiO_2 surfaces.[43] The adsorption energy is calculated to be 0.89 eV (Table 2), which is much higher than the value of 0.21 eV (-20.08 kJ mol^{-1}) reported in previous work,[44] in which the CO molecule weakly interacts with titanium ion in the physical adsorption mode.

The cases on FTs are different. On F_IT, the preferred adsorption configuration of CO is it bonds perpendicularly to Ti_{5C} atom, which is adjacent to F atom, with a slight slope on the surface through connection of C atom and Ti atom (see Figure 5b). The adsorption energy is 0.36 eV. This weak adsorption indicates that it is physisorption. A relatively weak adsorption confirms that activity of the surface is reduced after O_{2C} is replaced by F ions. Experimental works[10, 45] reported that doping of fluorine ions also raises the stabilization of (001) facet. This is likely due to O atom on the surface, which is undercoordinated and has a relatively high activity. When O_{2C} atom is

replaced by F dopants, the 2p orbitals of substitution F atom are fully occupied and hard to hybridize with C atom of CO. While the configurations of CO on $F_{II}T$ and $F_{III}T$ are similar to PT (Figures 5c, d), both are chemisorptions. The adsorption energies are close to or higher than PT. These results indicate that the promotive effects upon CO adsorptions mainly occur on the surface with a deeper F ions doping.

Bader charge analysis (Table 2) shows that CO acts as an electron acceptor on F_IT, however, it acts as an electron donor on other surfaces. In cases of donation of electrons to the surfaces, the charge transfer on FTs is smaller than on PT. This may be due to the Fermi level raised by F-dopant making it harder to donate electrons to the surfaces. To further understand the mechanism of CO adsorptions, the PDOS analysis is presented. From Figure 6 (b, d and e), we observe that in chemisorption (on PT, $F_{II}T$ and $F_{III}T$), the bonding orbital 5σ (HOMO) mixes with the states of substrate in valence band. Generally, bonding of CO molecule to a substrate can be characterized by a two-way electron flow involving both donation from CO 5σ orbital into empty orbitals of exposed Lewis acid sites (Ti_{5C}) and back donation from surface states to CO $2\pi^*$ empty orbitals, namely, the so-called σ-donation/π-back donation mechanism,[46] in which the HOMO and LUMO of CO hybridize with d orbitals of transition-metal atom in an appropriate energy range. In chemisorption (on PT, $F_{II}T$ and $F_{III}T$), a definitely positive net charge of adsorbed CO and reduction of Lewis acid site charge (-0.09~-0.1) combined with charge reduction (-0.55~-0.58) on O_{2C} which bonds to C atom indicate that the mechanism of σ-donation dominates the interaction. This is in tune with the result of interaction of CO with Ti_2O_3 $(10\bar{1}2)$

surface, though CO on this surface has a C-down configuration.[42b] Accordingly, CO 5σ state is significantly stabilized (3~4 eV) after the interaction, becoming almost degenerate with CO 1π states. The states at the top of valence band (VB) are derived from the formation of σ bond between C atom and O_{2C}, accompanied by donation of electrons to the O_{2C}. This donation, combined with 5σ donation, makes the net charge of adsorbed CO a significant growth (Table 2). The CO $2\pi^*$ empty level is perturbed to a very limited extent (0.1~1 eV), revealing a weak π-back donation. Though the π-back donation is small, the bond length or r(C-O) is elongated by 11% with reference to the free CO molecule (from 1.14 to 1.27Å). This has substantiated Lupinetti et al.[42c] who reported that a relatively small amount of back donation from the Lewis acid site to CO is sufficient to lengthen the CO bond. In FTs, donation of electron from CO to substrate keeps the state of Ti^{3+} in the band gap. The donor behavior of CO molecule was also observed on the surface of other transition metal oxides.[42d, 42e]

In the case of physisorption (on F_IT, Figure 5b), adsorption of CO has a C-down oriented configuration atop the Lewis acid site. The negative charge of adsorbed CO and charge reduction on the Lewis acid site (-0.20) indicate that both σ-donation and π-back donation mechanisms contribute to CO/F_IT bonding. In fact, the two-way electron flow process is the main interaction mechanism in C-down oriented configuration in transition metal oxides.[42a, 42b] With inspection of PDOS (Figure 6c), one can find that both 5σ and $2\pi^*$ states of CO have been stabilized upon the adsorption. Balancing the two opposite effects, the adsorbed CO gets a negative net

charge of -0.067. This charge reduction indicates that π-back donation is more efficient than σ-donation. Thus, the adsorbed CO acts as an electron acceptor in this case. This is mainly due to the substitution of O_{2C} atom by F ions, for which it is hard to participate in hybridization, which in turn makes the upright configuration more favorable. Thus, the LUMO orbital plays a major role in this configuration and makes π-back donation more favorable. Rohrbach et al.[46] reported that CO can be adsorbed on NiO surface in an upright configuration via π-back donation, in which electrons transfer from d orbitals of metal to $2\pi^*$ orbital of CO. The adsorption of CO in C-down oriented configuration on V_2O_3 $(10\bar{1}2)$ also has a main characteristic of π-back donation.[42a, 42b] In the interaction of CO/F_ITs, a small charge transfers from substrate to CO molecule has little effect on Ti^{3+}. Thus, the state of Ti^{3+} can be reserved in the band gap upon adsorption and magnetic moment of the system remains unchanged. Like the case of O_2, the most preferable adsorption of CO occurs on F_{III}T. It gives a smaller amount of electron donation to the substrate as compared to on PT (Table 2), this may be because the Fermi level with a higher location in band gap weakens the electron transfer from CO to the substrate.

Table 2: Relaxed structural parameters (bond lengths), charge transfers (ΔQ), magnetic moments (M) and adsorption energies (E_{ads}) of CO molecule in gas phase and most stable adsorptions.

Gas/Substrate	C-O_s(Å)	C-Ti_s(Å)	O-Ti_s(Å)	C-O(Å)	ΔQ(|e|)	M(μ_B)	E_{ads} (eV)
CO (gas phase)	-	-	-	1.142	-	0	-
CO/PT	1.291	2.072	2.089	1.269	0.664	0	0.89
CO/F_IT	-	2.330	-	1.143	-0.067	1.0	0.36
CO/F_{II}T	1.297	2.077	2.095	1.266	0.656	1.0	0.86
CO/F_{III}T	1.302	2.093	2.094	1.266	0.628	1.0	1.07

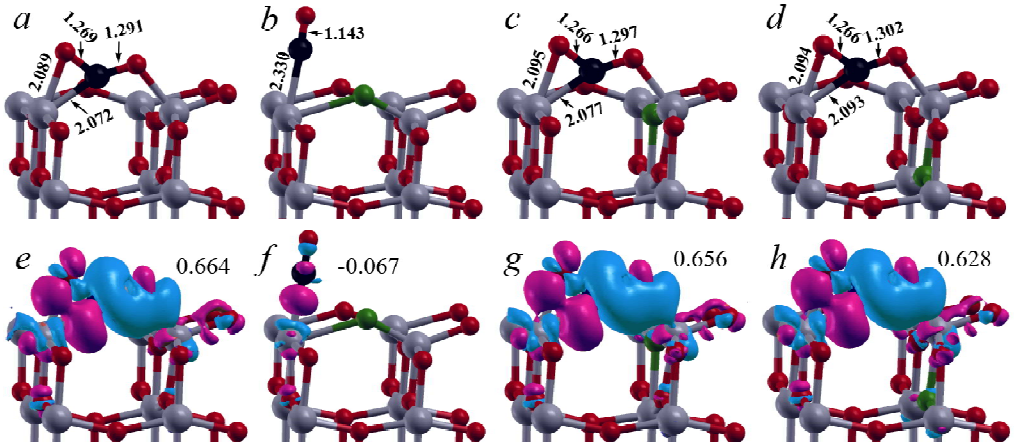

Figure 5: Optimized adsorption geometries and charge transfer of CO molecule on pristine and F-doped surfaces in the most stable configurations. The upper panel shows adsorption geometries of CO on: (a) pristine; (b) F_I-doped; (c) F_{II}-doped; and (d) F_{III}-doped surface; the lower panel (e~h) shows the corresponding charge transfer between them. The isosurface value is 0.005 e/bohr^3. The black sphere represents C atom. A negative value of charge transfer indicates that the molecule gains electrons from the surface and vice versa.

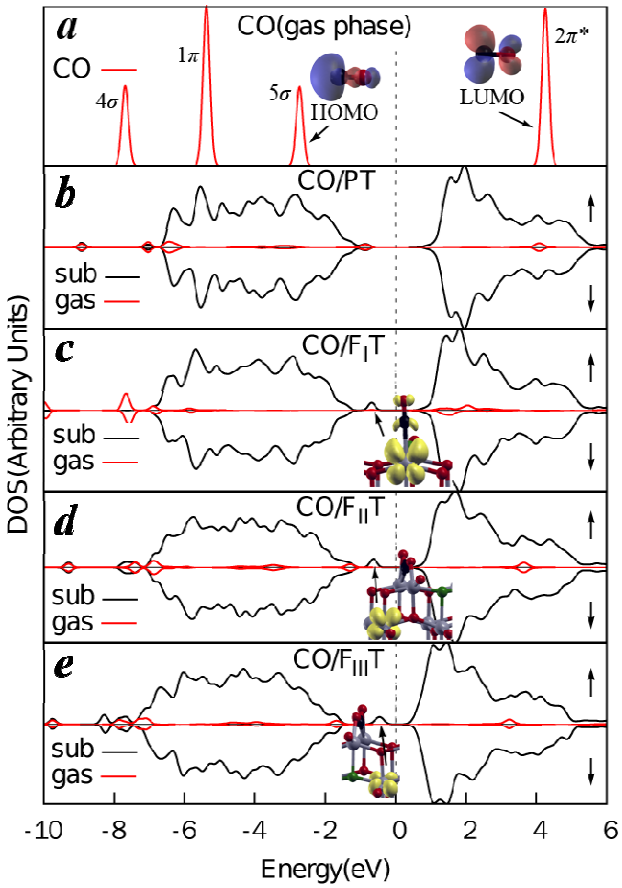

Figure 6: (a) TDOS for a gas-phase CO molecule; PDOS for CO on (b) pristine, (c) F_I-doped, (d) F_{II}-doped and (e) F_{III}-doped anatase (001) surface. Insets show the location of spin polarized electrons. The Fermi level is set to zero.

3.2.3 NO adsorption

NO has been reported to have an interactional mechanism similar to that of CO molecule on transition-metal oxides.[47] In our calculation, the most stable adsorption of NO on PT is a lying-down configuration, in which O atom bonds to Ti_{5C} and N bonds to O_{2C}, with N-O bond lying nearly parallel to the surface in [100] direction (Figure 7a). The adsorption energy is calculated to be 0.47 eV (Table 3). The bond length of O-Ti_{5C} and N-O_{2C} is 2.038 Å and 1.355 Å, respectively. The bond lengths

show that the molecule is close enough to the surface to form chemical bonds, implying it is chemisorption. While on FTs, the most stable adsorptions are upright configurations, in which N atom bonds to Ti_{5C}, with the molecule nearly perpendicular to the surface (shown in Figure 7b~d). On FTs, larger adsorption energies of NO indicate that the adsorptions have been distinctly enhanced. Among the three FTs, NO on $F_{III}T$ has the strongest adsorption, with adsorption energy of 1.07 eV (Table 3), and it has the shortest molecule-substrate distance of 1.951 Å. The charge transfers on FTs are also distinctly greater than on PT (Figure 7e~h).

Figure 8 shows PDOS of NO molecule adsorption on PT and FTs. Figure 8b shows that the occupied 5σ orbital of NO is broadened and is strongly hybridized with d orbital having an electron donation from NO 5σ to Ti 3d orbitals (Figure 8b). This donation increases the charge on Ti_{5C} and consequently a state of Ti^{3+} appears in the band gap. Meanwhile, it is accompanied by a relatively weak back donation from Ti 3d (d_z^2) to partially occupied $2\pi^*$ anti-bonding orbital. On the other hand, significant charge depletion on O atom bonding with N atom leads to an increased filling of $2\pi^*$ anti-bonding orbital. As a consequence, NO carries a net charge of -0.144 and the bond length of N-O has been elongated from 1.167 Å (in gas phase) to 1.284 Å. The redistribution of electron makes the system have a magnetic moment of 1 μ_B (shown in inserted panel of Figure 8a.). Integrated over NO molecule, although both donation and back donation mechanisms contribute to NO/PT bonding, π-back donation is slightly more efficient than σ-donation. This is different from the case of CO/PT bonding, in which σ-donation plays the major role. This difference originates from the

fact that free NO $2\pi^*$ orbital (HOMO) is lower in energy than CO $2\pi^*$ which is the lowest unoccupied MO (LUMO).[42d, 42e] Thus, NO behaves as an electron acceptor in the interaction of NO/PT.

Pertaining to the adsorption on FTs, NO of the most stable adsorption has N-down oriented configuration atop the Lewis acid site. The negative net charge of the adsorbed NO molecules, combined with charge reduction on the Lewis acid site (-0.09~0.11), reveal that both σ-donation and π-back donation mechanisms contribute to the bonding of NO/FTs. The negative net charge of adsorbed NO indicates that π-back donation is more efficient than σ-donation. With inspection of PDOS analysis (Figure 8c~e), we can see that there is a strong Ti 3d-$2\pi^*$ hybridization in which electrons are back donated from d_{xy} to $2\pi^*$ orbital, which causes the state of Ti 3d (d_{xy}) to disappear. This hybridization makes the overlapped Ti^{3+} states broader than the original Ti^{3+} states, and the gap becomes narrower. After accepting the electrons, the $2\pi^*$ anti-bonding orbital shifts to nearly below the Fermi level, overlapping with the localized states of Ti^{3+}. Meanwhile, there exists a relatively weak hybridization between 5σ orbital of NO and Ti 3d orbitals (5σ-donation). This donation results in another Ti 3d (d_z^2) state appearing in the band gap. A larger degree of $2\pi^*$ back donation makes the net charge of NO gained from the surface greater than on PT (Figures 7e~h). This process of 5σ-donation/$2\pi^*$-back donation causes the system to have a magnetic moment of $2\mu_B$ (Table 3). This is mainly due to the existence of excess electrons induced by F-dopants having raised the Fermi level and enhanced the $2\pi^*$-back donation process, which makes the upright configuration more favorable. A

lower Fermi level makes 5σ-donation more favorable and causes a lying-down configuration. This is probably the major source that NO has different stable configurations on PT and FTs. The mechanism of 5σ-donation and 2π^*-back donation of NO was also observed on other oxides.[47] Bonding of NO/FTs has an interaction mechanism similar to CO/F_IT interaction, in which the adsorbed CO has a C-down oriented configuration and a main interaction mechanism of π-back donation. However, a much larger net charge on adsorbed NO reveals that π-back donation mechanism is more efficient in NO than in CO. This is derived from the same nature that HOMO of free NO is lower in energy than LUMO of CO. These results are perfectly in tune with the behaviors of NO on other transition metal oxides such as Cu_2O and Ag_2O.[42d, 42e]

Table 3: Relaxed structural parameters (bond lengths, angle), charge transfer (ΔQ), magnetic moments (M) and adsorption energies (E_{ads}) of NO molecule in gas phase and most stable adsorptions.

Gas/Substrate	N-O_s(Å)	O-Ti_s(Å)	N-Ti_s(Å)	N-O(Å)	∠O-N-Ti_s(°)	ΔQ(|e|)	M(μ_B)	E_{ads} (eV)
NO (gas phase)	-	-	-	1.167	-	-	1.0	-
NO/PT	1.355	2.038	2.823	1.284	-	-0.144	1.0	0.47
NO/F_IT	-	-	1.966	1.187	177.49	-0.317	2.0	0.97
NO/F_{II}T	-	-	1.994	1.184	172.73	-0.297	2.0	0.87
NO/F_{III}T	-	-	1.951	1.187	178.31	-0.324	2.0	1.07

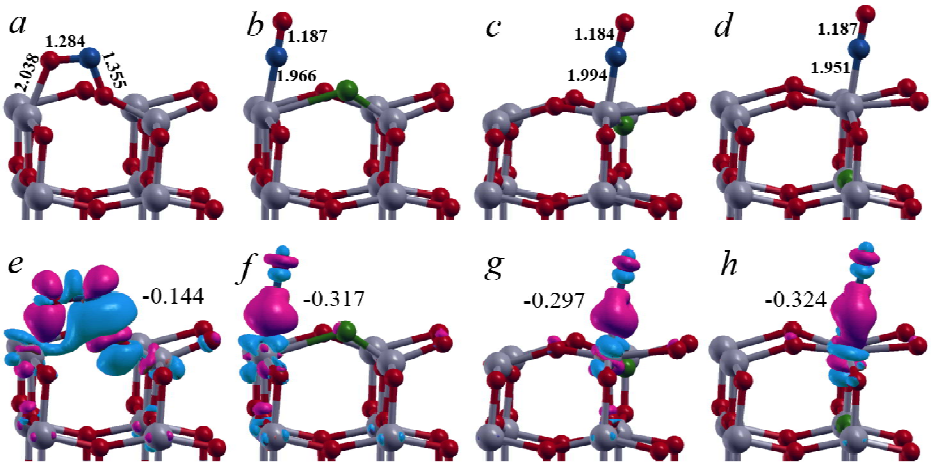

Figure 7: Optimized adsorption geometries and charge transfer of NO molecule on pristine and F-doped surfaces in the most stable configurations. The upper panel shows adsorption geometries of NO on: (a) pristine; (b) F_I-doped; (c) F_{II}-doped; and (d) F_{III}-doped surface; the lower panel (e~h) shows the corresponding charge transfer between them. The dark blue sphere represents N atom. The isosurface value is set at 0.005 e/bohr^3.

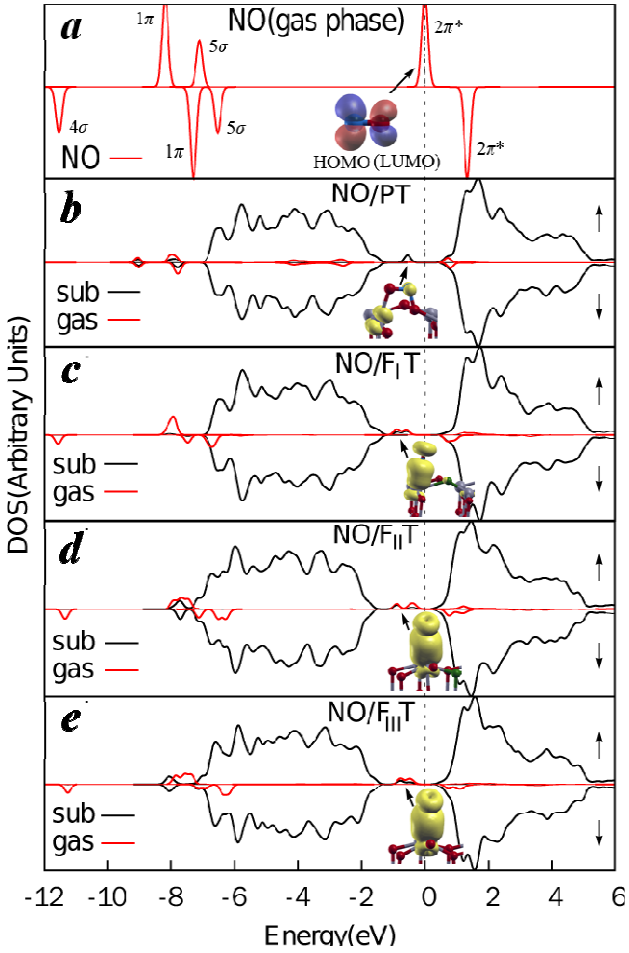

Figure 8：(a) TDOS for a gas-phase NO molecule; PDOS for NO on (b) pristine, (c) F_I-doped, (d) F_{II}-doped, and (e) F_{III}-doped anatase (001) surface. Insets show the location of spin polarized electrons. The Fermi level is set to zero.

3.2.4 NO_2 adsorption

NO_2, another toxic and irritating gas produced in power generation and internal combustion engines of automobiles, causes serious environmental problems such as forming of acid rain and destruction of the ozone layer. Investigation of interaction of NO_2 with TiO_2 is meaningful for exploring efficient technologies to trap or destroy NO_x species for prevention of environmental pollution. Therefore, we further

investigated the adsorption of NO_2 on PT and FTs. For adsorption of NO_2, the most favorable way to interact with PT is an η^2-N,O configuration, in which the molecule is adsorbed on the surface via N bonds to O_{2C} and O bonds to Ti_{5C}, and another O atom of NO_2 is upward to N atom with a tilt of the N-O bond (Figure 9a). The adsorption energy is calculated to be 0.35 eV. The bond lengths of N-O_{2C} and O-Ti_{5C} are 1.333 and 2.151 Å, respectively, implying chemical bonds have been formed. Like NO adsorption on PT, adsorption of NO_2 on PT also induces a magnetic moment of 1 μ_B to the molecule-substrate system. This is because the unpaired electron in 6a1 orbital transfers to the substrate and forms Ti^{3+}.

The most stable adsorption of NO_2 on FTs is an η^2-O,O configuration, in which NO_2 bonds with two adjacent Ti_{5C} atoms via two O atoms to form a bidentate configuration, with molecules crossing above the surface O_{3C} atom (shown in Figure 9b~d). This bidentate adsorption mode of NO_2 is usually the most stable configuration found on other metallic oxide surfaces, such as Al_2O_3[48] and ZnO.[38b] Configurations of NO_2 on the three kinds of FTs are similar. The adsorption of NO_2 on FTs is found to be much stronger than on PT. The adsorption energies on F_IT, $F_{II}T$ and $F_{III}T$ were calculated to be 2.00, 2.08 and 2.27 eV (Table 4), respectively, showing that F-dopants significantly enhance adsorption. Interestingly, magnetic moment which was found to be 1 μ_B in adsorption on PT vanished (0 μ_B) in all F-doped substrate adsorption systems.

Electronic structure of NO_2 adsorption on PT and FTs are shown in Figure 10. The partially occupied spin-down component of 6a1 orbital (HOMO/LUMO) is

slightly higher than the Fermi level of PT. This induces a charge transfer to the substrate when adsorption takes place on PT. The unpaired electron transfers from this orbital to Ti 3d orbital and produces Ti^{3+} state in the band gap (Figure 10b), which is also the origin of magnetic moment 1 μ_B of the system. On the other hand, O atom interacts with Ti_{5C} atom and induces σ-bond formed between them. This causes a charge transfer from 3d orbital of Ti_{5C} to O 2p orbital. As a result, NO_2 molecule has a slightly negative net charge of -0.069 (Table 4).

In FTs, F-dopants make the surfaces n-type doped and lift the Fermi level to the bottom of CB. This makes LUMO of NO_2 lower than the Fermi level. Thus, the NO_2 molecule becomes a good electron acceptor and an oxidizing agent for excess electrons induced surfaces. Therefore, a large charge transfer from the surface to the molecule occurs when it reacts with Ti atom. The molecules on F_IT, $F_{II}T$ and $F_{III}T$ gain charges of -0.647, -0.654 and -0.648, respectively; all are much greater than the charge transfer on PT (Table 4). After excess electrons flow to the molecule, the localized Ti^{3+} states induced by F-dopants disappear and the state of 6a1 becomes fully filled and falls down to the top of VB (Figure 10c~e). Therefore, the electron transfer makes the magnetic moment of molecule-substrate vanish and the band gap becomes broader. These significant changes of magnetic and electronic structure can be considered as switch signals in NO_2 detection applications.

Table 4: Relaxed structural parameters (bond lengths, angle), charge transfer (ΔQ), magnetic moments (M) and adsorption energies (E_{ads}) of NO_2 molecule in gas phase and most stable adsorptions.

Gas/Substrate	O(1)-Ti_s(Å)[a]	O(2)-Ti_s(Å)[a]	O(1)-N(Å)	O(2)-N(Å)	∠O(1)-N-O(2)(°)	ΔQ(|e|)	M(μ_B)	E_{ads} (eV)
NO_2 (gas phase)	-	-	1.212	1.212	133.64	-	1.0	-
NO_2/PT	-	2.151	1.217	1.289	126.50	-0.069	1.0	0.35
NO_2/F_IT	2.068	2.118	1.281	1.261	118.34	-0.647	0	2.00
NO_2/F_{II}T	2.067	2.066	1.268	1.269	116.95	-0.654	0	2.08
NO_2/F_{III}T	2.033	2.094	1.279	1.260	118.04	-0.648	0	2.27

[a] The labels of O atoms are shown in Figure 9.

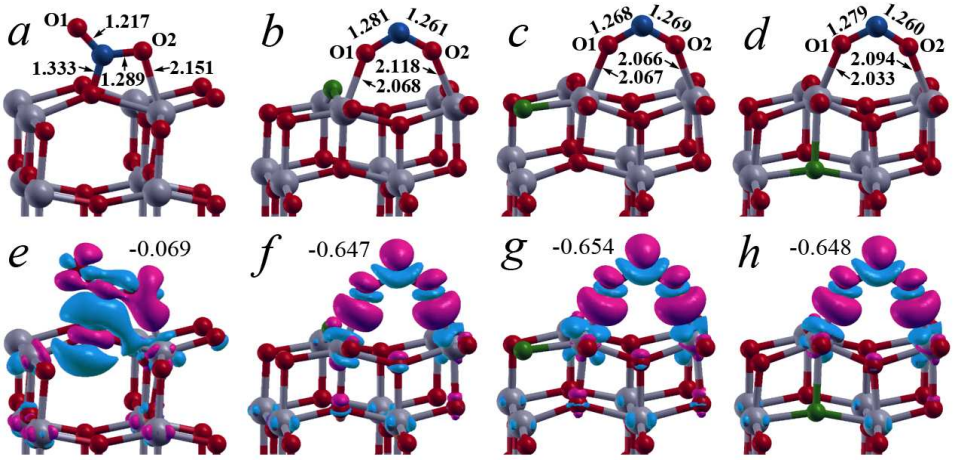

Figure 9: Optimized adsorption geometries and charge transfer of NO_2 molecule on pristine and F-doped surfaces in the most stable configurations. The upper panel shows adsorption geometries of NO_2 on: (a) pristine; (b) F_I-doped; (c) F_{II}-doped; and (d) F_{III}-doped surface; the lower panel (e~h) shows the corresponding charge transfer between them. The isosurface value is 0.005 e/bohr^3. The blue sphere represents N atom.

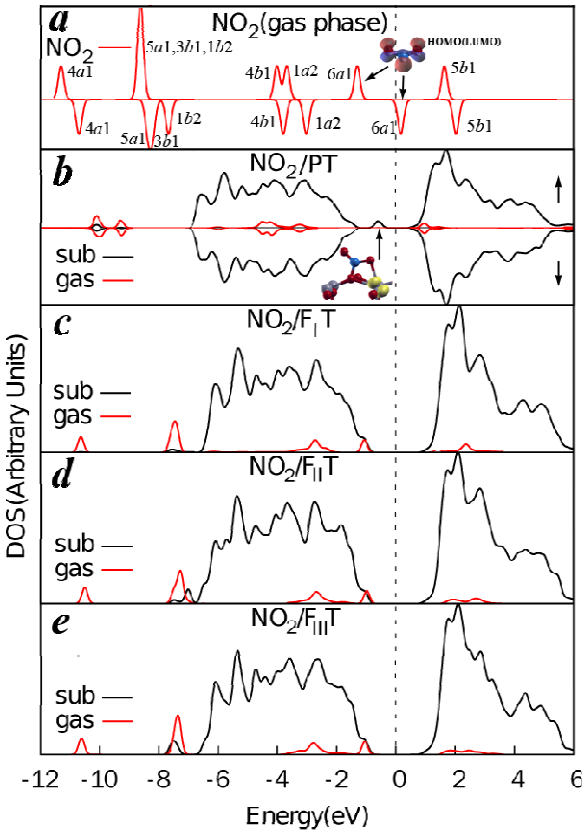

Figure 10：(a) TDOS for a gas-phase NO_2 molecule; PDOS for NO_2 on (b) pristine, (c) F_I-doped, (d) F_{II}-doped and (e) F_{III}-doped anatase (001) surface. Insets show the location of spin polarized electrons. The Fermi level is set to zero.

3.2.5 SO_2 adsorption

Sulfur dioxide (SO_2), a hazardous pollutant generated by combustion of coal and petroleum products, causes serious problems, including tremendously damaging effects of acid rain on ecology, hazards to human health and corrosion of monuments or buildings, etc.[49] Investigation of SO_2 with TiO_2 is of potential importance for degrading this poisonous gas. Importantly, TiO_2 is the most common catalyst used in chemical industry and oil refineries for degradation of SO_2 through $2H_2S + SO_2 \rightarrow$

$2H_2O + 3S\downarrow$ Claus reaction.[12, 49b, 50] Though interaction of adsorbed SO_2 complexes with rutile TiO_2 (110) has been extensively investigated experimentally[51] and theoretically,[49b, 52] investigation of SO_2 on pristine or F-doped anatase (001) in periodic surface model, especially from the level of analysis of the adsorbate-substrate bonding scheme, is lacking. Therefore, we performed the calculation of SO_2 on pristine and F-doped (001) surface.

In the most stable configuration of SO_2 on PT, SO_2 bonds with the surface via S atom bonds to O_{2C} and one of O atoms bonds to Ti_{5C} to form an η^2-S,O configuration,[53] a SO_3-like surface complex, leaving other O atom slanted upward on S atom (shown in Figure 11a). It is worth mentioning that SO_3 complex was believed to connect with dissociation of SO_2 to S.[50, 52a] The adsorbed SO_2 distorts the surface greatly and the bond O_{2C}-Ti_{5C} is broken. The symmetric S-O and O-Ti bonds in SO_3 structure are calculated to be 1.62~1.64 and 1.82~1.84 Å, respectively. The upward S-O bond is 1.461 Å, which is slightly longer than 1.458 Å in gas phase. The adsorption energy is 1.31 eV, implying it is a typical chemisorption. Similar to the adsorption on PT, the adsorption of SO_2 on $F_{II}T$ and $F_{III}T$ has also formed an η^2-S,O configuration, in which the molecule interacts with the surface via S bonds to O_{2C} and O bonds to Ti_{5C} (see Figures 11c~d). The adsorption energies on $F_{II}T$ and $F_{III}T$ are 1.28 and 1.60 eV, respectively, showing the F_{III}-dopant strongly enhancing the adsorption. Whereas the adsorption of SO_2 on F_IT forms an η^2-O,O configuration (shown in Figure 11b), in which SO_2 bonds with two adjacent Ti_{5C} atoms via two O atoms, similar to the configuration of NO_2 on FTs. The adsorption energy of this

configuration is 1.27 eV. The η^2-S,O configuration of SO_2 on FIT also exists, but it is much weaker than the former one and only has an adsorption energy of 0.47eV.

The adsorption mechanism (Figure 12) of a triangular-shaped SO_2 molecule on transition metallic oxides also involves σ-donation (electrons transfer from the occupied 8a1, 5b2 orbitals of SO_2 to the d orbitals of transition-metal atom) and π-back donation (electrons transfer from the metal or oxide to the empty 3b1 orbital of SO_2).[53] The process of σ-donation/π-back donation was considered to be the main mechanism of interaction on TiO_2[52a] and other oxides (or metal).[53-54]

Inspection of PDOS of η^2-S,O configuration (SO_2 on PT, $F_{II}T$ and $F_{III}T$), we found that adsorption on these surfaces has a similar mechanism (Figure 12). The strong hybridization of 4b2, 5b2, 8a1 and 3b1 orbitals of SO_2 with substrate states and negligible change (0.01~0.05) on the charge of the Lewis acid site reveals that both donation and back donation mechanisms contribute to the interactions. It was reported that interaction between SO_3 surface complex and rutile (110) surface has also a two-way electron flow michanism,[52a] implying the common character of SO_3/substrate interaction. The positive net charge on adsorbed SO_2 (Table 5) indicates that σ-donation is more efficient than π-back donation. This may be ascribed to the interaction mechanism being dependent upon the molecular orbitals with the proper symmetry, energy and spatial extension to overlap with substrate orbitals.[55] In the η^2-S,O configuration, lobes of 8a1 have an extension in perpendicular orientation, facilitating the overlap with Ti 3d orbitals. So it is reasonable to foresee the major role of σ-donation in this perpendicular configuration. The character of charge transfers

from SO_2 to substrate and the dominant role of σ-donation in the interaction of η^2-S,O configuration reconcile with previous works theoretically[56] and experimentally.[57] On $F_{II}T$ and $F_{III}T$, the supplement of electrons makes the Ti^{3+} states remain within the band gap (Figure 12d, e). This results in the two adsorption systems having a magnetic moment of 1 μ_B.

In η^2-O,O configuration (SO_2 on F_IT), two O atoms of SO_2 bond to the surface Ti atoms. It may be due to the inactivation effects and ionic features of F-dopant, which means the S atom of SO_2 can hardly hybridize with it. This makes SO_2 interact with the two adjacent Ti atoms via two O atoms by crossing it to form a η^2-O,O bridge configuration. As a result, the LUMO of SO_2 is able to hybridize with Ti 3d orbitals quite well, due to its unique shape. The electron in Ti 3d orbitals flows to π^* orbital to form π-back donation. In this process, the 3b1 state splits into two parts and becomes partially occupied: one part locates below the Fermi level, and the other locates below the bottom of CB (Figure 12c). The charge transfer depletes the excess electron in Ti^{3+} and diminishes the state of Ti^{3+} in the band gap. Instead, a new polarized state of π^* orbital appears below the Fermi level. The polarized π^* state induces a magnetic moment of 1 μ_B to the system. As a result, SO_2 has a negative net charge of -0.637 that resulted from withdrawal of electrons from the surface (Table 5).

Like the cases of other molecules, adsorption of SO_2 on $F_{III}T$ also has the highest adsorption energy. It can be seen in Table 5 that in the cases of SO_2 on $F_{II}T$ or $F_{III}T$, the charge transfer is smaller than on PT, implying the existence of excess electrons induced by F-dopants can weaken σ-donation to some degrees. Thus, the molecule of

η^2-S,O configuration on FTs loses less charge than that on PT. The adsorption of SO_2 on F_IT causes a larger charge transfer than on other surfaces (PT, $F_{II}T$ and $F_{III}T$). But it has the lowest adsorption energy. This is caused by the serious deformation of Ti-F-Ti bridge structure. The molecule crosses upon F atom has forced the F atom down from its original location by 0.71 Å. This distortion raises the system energy and weakens the interaction. As a result, the adsorption energy of SO_2 on F_IT is lower than on other surfaces. These results indicate that F-dopants at different depths in the surface can affect the configurations and orientation of the adsorbed molecule and have different effects on the mechanism of charge transfer.

Table 5: Relaxed structural parameters (bond lengths, angle), charge transfer (ΔQ), magnetic moments (M) and adsorption energies (E_{ads}) of SO_2 molecule in gas phase and most stable adsorptions.

Gas/Substrate	O(1)-Ti_s(Å)[a]	S-O_s/O(2)-Ti_s(Å)[a,b]	O(1)-S(Å)	O(2)-S(Å)	∠O(1)-S-O(2)(°)	ΔQ(|e|)	M(μ_B)	E_{ads} (eV)
SO_2 (gas phase)	-	-	1.212	1.212	119.16	-	0	-
SO_2/PT	1.843	1.639	1.621	1.461	107.33	0.413	0	1.31
SO_2/F_IT	2.065	2.051	1.539	1.542	116.22	-0.637	1.0	1.27
$SO_2/F_{II}T$	1.902	1.686	1.610	1.462	108.73	0.350	1.0	1.28

[a] The labels of O atoms are shown in Figure 11.

[b] In the case of SO_2/F_IT, the data refers to O(2)-Ti_s; while in other cases, the data refers to S-O_s.

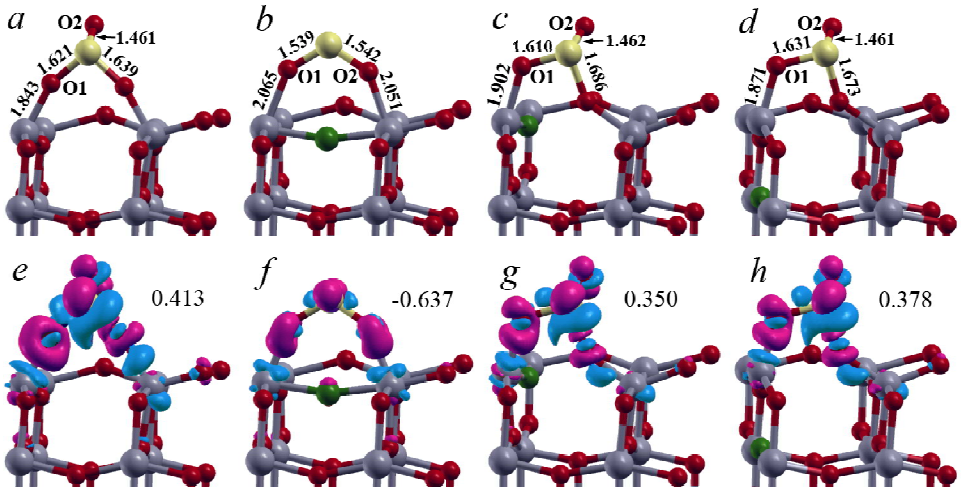

Figure 11: Optimized adsorption geometries and charge transfer of SO_2 molecule on pristine and F-doped surfaces in the most stable configurations. The upper panel shows the adsorption geometries of SO_2 on: (a) pristine; (b) F_I-doped; (c) F_{II}-doped; and (d) F_{III}-doped surface; the lower panel (e~h) shows the corresponding charge transfer between them. The isosurface value is 0.005 e/bohr^3. The yellow sphere represents S atom.

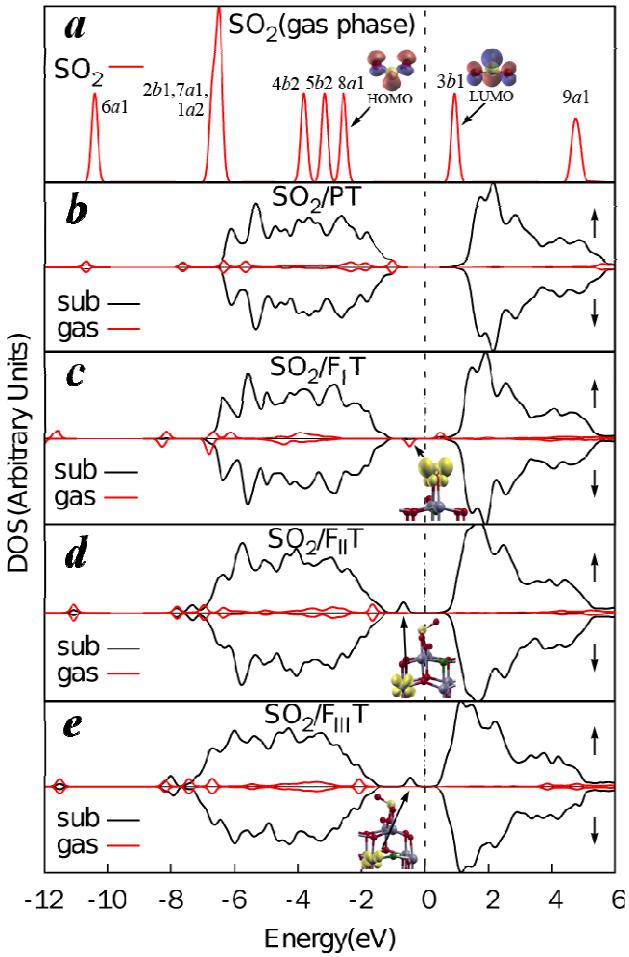

Figure 12：(a) TDOS for a gas-phase SO_2 molecule; PDOS for SO_2 on: (b) pristine, (c) F_I-doped, (d) F_{II}-doped, and (e) F_{III}-doped anatase (001) surface. Insets show the location of spin polarized electrons. The Fermi level is set to zero.

4 Conclusions

In this work, we have performed DFT calculations to study the structural and electronic properties of several gas molecules (O_2, CO, NO, NO_2 and SO_2) on pristine and F-doped anatase TiO_2 (001) surfaces. Different surface energies show that the three F-dopants have different effects on properties of TiO_2. The results indicate that F_I dopant reduces activity while F_{III} increases activity of the TiO_2 surface, and F_{II}

induces surface activity close to that of the pristine one. We found that the surface energies are not the only factor which affects the surface properties. In F-doped surfaces, another important factor is the F-dopant induced excess electron which is fully localized in a 3d orbital of Ti^{3+}. The existence of this electron induced a defect state below the bottom of CB about 0.8~1.1 eV. The defect states induced by three kinds of F-dopants were found to have a significant promotion on the adsorption of O_2, NO and NO_2. However, the promotive effect of F_I and F_{II} dopants was not found upon the adsorption of CO and SO_2. For these two molecules, only F_{III} dopant was found to have the promotive effect. These results show that doping with F ions would promote the adsorbability of TiO_2 surface for oxidative gas molecules which has a tendency to capture electrons in reactions.

Among different gas molecules, O_2 and NO_2 have a similar interaction mechanism upon adsorption. Both interact with the surface through charge transfer process because their Fermi levels are within an appropriate range in the band gap of the surfaces. The main feature is that the adsorption is accompanied by a significant charge transfer. As compared to PT, the existence of excess electrons induced by F-dopants can raise the quantity of transferred electrons and make the adsorption stronger. Especially for O_2 adsorption, which cannot occur spontaneously on PT at all, strongly takes place on FTs. In this process, Ti^{3+} takes on a key role in electron transfer from the surface to O_2 molecule. Also, adsorptions of both kinds of molecules can diminish the state of Ti^{3+} in band gap, showing they have a strong electrophilic property. CO, NO and SO_2 have the main interaction mechanism of σ-donation and

π-back donation hybridization processes, which involve the electrons transfer from the occupied σ orbital of the molecule to the d orbitals of transition metallic atom, or electrons transfer from the d orbitals of metal or oxide into the empty π orbital of the molecule. The main feature is that the adsorption is accompanied by hybridization of σ or π states with the surface Ti 3d orbitals. On FTs, the existence of Ti^{3+} has an effect on the molecular orientation in adsorptions and results in a different adsorption style. For example, in adsorption of CO or SO_2 on F_IT, π-back donation plays the major role; however, on $F_{II}T$ or $F_{III}T$, σ-donation plays the major role. Thus the configurations in these cases are different. In contrast with CO-substrate bonding, π-back donation is more efficient than σ-donation in all NO-substrate interactions in the most stable configurations.

The study shows that Ti^{3+} has some unique effects on not only electronic and magnetic properties but also configuration of the adsorbed gases. The findings provide an important explanation for a better understanding of the effects of F-dopants in improving the performance of TiO_2 surfaces. The bridge role of Ti^{3+} induced by F-dopants in electron transferring and enhancing effects on adsorptions of oxidative gas molecules suggests the great potential of this species for future applications of titania-based catalyst.

Acknowledgements

This research was fully supported by the Research Grants Council of the Hong Kong Special Administrative Region, China (Project No: 9042047, CityU 11208914). We also gratefully acknowledge the computing support from CETV and guoshi.com for High-Performance Computing. In addition, the first author would like to thank Dr Y. K. Lei for his fruitful discussion.

References

1 (a) A. Fujishima and K. Honda, *Nature*, 1972, **238**, 37-38; (b) M. R. Hoffmann, S. T. Martin, W. Choi and D. W. Bahnemann, *Chem. Rev.*, 1995, **95**, 69-96; (c) S. U. M. Khan, M. Al-Shahry and W. B. Ingler, *Science*, 2002, **297**, 2243-2245; (d) M. Gratzel, *Nature*, 2001, **414**, 338-344; (e) J. H. Park, S. Kim and A. J. Bard, *Nano Lett*, 2006, **6**, 24-28; (f) X. Z. Li and F. B. Li, *Environ. Sci. Technol.*, 2001, **35**, 2381-2387; (g) H. Choi, M. G. Antoniou, M. Pelaez, A. A. de la Cruz, J. A. Shoemaker and D. D. Dionysiou, *Environ. Sci. Technol.*, 2007, **41**, 7530-7535; (h) H. Tang, K. Prasad, R. Sanjinés and F. Lévy, *Sens. Actuators, B*, 1995, **26**, 71-75; (i) E. Traversa, *Sens. Actuators, B*, 1995, **23**, 135-156.

2 X. Chen and S. S. Mao, *Chem. Rev.*, 2007, **107**, 2891-2959.

3 (a) J. Yu, Q. Xiang and M. Zhou, *Appl. Catal., B*, 2009, **90**, 595-602; (b) B. Liu, X. Wang, G. Cai, L. Wen, Y. Song and X. Zhao, *J. Hazard. Mater.*, 2009, **169**, 1112-1118.

4 R. Asahi, T. Morikawa, T. Ohwaki, K. Aoki and Y. Taga, *Science*, 2001, **293**, 269-271.

5 H. Irie, Y. Watanabe and K. Hashimoto, *J. Phys. Chem. B*, 2003, **107**, 5483-5486.

6 T. Ohno, M. Akiyoshi, T. Umebayashi, K. Asai, T. Mitsui and M. Matsumura, *Appl. Catal., A*, 2004, **265**, 115-121.

7 N. Lu, X. Quan, J. Li, S. Chen, H. Yu and G. Chen, *J. Phys. Chem. C*, 2007, **111**, 11836-11842.

8 (a) J. C. Yu, J. Yu, W. Ho, Z. Jiang and L. Zhang, *Chem. Mater.*, 2002, **14**,

3808-3816; (b) S. Liu, J. Yu and W. Wang, *Phys. Chem. Chem. Phys.*, 2010, **12**, 12308-12315.

9 N. Todorova, T. Giannakopoulou, T. Vaimakis and C. Trapalis, *Mater. Sci. Eng., B*, 2008, **152**, 50-54.

10 (a)H. G. Yang, C. H. Sun, S. Z. Qiao, J. Zou, G. Liu, S. C. Smith, H. M. Cheng and G. Q. Lu, *Nature*, 2008, **453**, 638-641; (b) X. Han, Q. Kuang, M. Jin, Z. Xie and L. Zheng, *J. Am. Chem. Soc.*, 2009, **131**, 3152-3153.

11 (a) A. Vittadini, A. Selloni, F. P. Rotzinger and M. Grätzel, *Phys. Rev. Lett.*, 1998, **81**, 2954-2957; (b) M. Lazzeri, A. Vittadini and A. Selloni, *Phys. Rev. B*, 2001, **63**, 155409; (c) U. Diebold, N. Ruzycki, G. S. Herman and A. Selloni, *Catal. Today*, 2003, **85**, 93-100; (d) A. Vittadini, M. Casarin and A. Selloni, *Theor. Chem. Acc.*, 2007, **117**, 663-671; (e) M. Palummo, G. Giorgi, L. Chiodo, A. Rubio, and K. Yamashita, *J. Phys. Chem. C,* 2012, **116**, 18495-18503; (f) X.-Q. Gong, A. Selloni and A. Vittadini, *J. Phys. Chem. B*, 2006, **110**, 2804-2811.

12 U. Diebold, *Surf. Sci. Rep.*, 2003, **48**, 53-229.

13 (a) J. Xu, Y. Ao, D. Fu and C. Yuan, *Appl. Surf. Sci.*, 2008, **254**, 3033-3038; (b) H. Yang and X. Zhang, *J. Mater. Chem.*, 2009, **19**, 6907-6914.

14 C. Di Valentin, G. Pacchioni and A. Selloni, *J. Phys. Chem. C,* 2009, **113**, 20543-20552.

15 D. Li, H. Haneda, N. K. Labhsetwar, S. Hishita and N. Ohashi, *Chem. Phys. Lett.*, 2005, **401**, 579-584.

16 H. A. Seibel Ii, P. Karen, T. R. Wagner and P. M. Woodward, *J. Mater. Chem.*,

2009, **19**, 471-477.

17 A. M. Czoska, S. Livraghi, M. Chiesa, E. Giamello, S. Agnoli, G. Granozzi, E. Finazzi, C. D. Valentin and G. Pacchioni, *J. Phys. Chem. C*, 2008, **112**, 8951-8956.

18 M. V. Ganduglia-Pirovano, A. Hofmann and J. Sauer, *Surf. Sci. Rep.*, 2007, **62**, 219-270.

19 V. I. Anisimov, I. V. Solovyev, M. A. Korotin, M. T. Czyżyk and G. A. Sawatzky, *Phys. Rev. B*, 1993, **48**, 16929-16934.

20 E. Finazzi, C. Di Valentin, G. Pacchioni and A. Selloni, *J. Chem. Phys.*, 2008, **129**, 154113.

21 (a) C. J. Calzado, N. C. Hernández and J. F. Sanz, *Phys. Rev. B*, 2008, **77**, 045118; (b) M. Arroyo-de Dompablo, A. Morales-García and M. Taravillo, *J. Chem. Phys.*, 2011, **135**, 054503.

22 (a) N. A. Deskins and M. Dupuis, *Phys. Rev. B*, 2007, **75**, 195212; (b) C. Persson and A. Ferreira da Silva, *Appl. Phys. Lett.*, 2005, **86**, 231912.

23 (a) J. Stausholm-Møller, H. H. Kristoffersen, B. Hinnemann, G. K. Madsen and B. Hammer, *J. Chem. Phys.*, 2010, **133**, 144708; (b) C. J. Calzado, N. C. Hernández and J. F. Sanz, *Phys. Rev. B*, 2008, **77**, 045118; (c) N. A. Deskins, R. Rousseau and M. Dupuis, *J. Phys. Chem. C,* 2011, **115**, 7562-7572.

24 G. Mattioli, F. Filippone, P. Alippi and A. Amore Bonapasta, *Phys. Rev. B*, 2008, **78**, 241201.

25 (a) V. I. Anisimov, J. Zaanen and O. K. Andersen, *Phys. Rev. B*, 1991, **44**, 943-954; (b) A. I. Liechtenstein, V. I. Anisimov and J. Zaanen, *Phys. Rev. B*, 1995, **52**,

R5467-R5470; (c) S. L. Dudarev, G. A. Botton, S. Y. Savrasov, C. J. Humphreys and A. P. Sutton, *Phys. Rev. B*, 1998, **57**, 1505-1509.

26 (a) Y. Wang and J. P. Perdew, *Phys. Rev. B*, 1991, **44**, 13298-13307; (b) J. P. Perdew, J. A. Chevary, S. H. Vosko, K. A. Jackson, M. R. Pederson, D. J. Singh and C. Fiolhais, *Phys. Rev. B*, 1992, **46**, 6671-6687.

27 P. Giannozzi, S. Baroni, N. Bonini, M. Calandra, R. Car, C. Cavazzoni, D. Ceresoli, G. L. Chiarotti, M. Cococcioni, I. Dabo, A. Dal Corso, S. De Gironcoli, S. Fabris, G. Fratesi, R. Gebauer, U. Gerstmann, C. Gougoussis, A. Kokalj, M. Lazzeri, L. Martin-Samos, N. Marzari, F. Mauri, R. Mazzarello, S. Paolini, A. Pasquarello, L. Paulatto, C. Sbraccia, S. Scandolo, G. Sclauzero, A. P. Seitsonen, A. Smogunov, P. Umari and R. M. Wentzcovitch, *J. Phys.: Condens. Matter.*, 2009, **21**.

28 D. Vanderbilt, *Phys. Rev. B*, 1990, **41**, 7892-7895.

29 (a) W.-F. Huang, H.-T. Chen and M. C. Lin, *J. Phys. Chem. C,* 2009, **113**, 20411-20420; (b) J. K. Burdett, T. Hughbanks, G. J. Miller, J. W. Richardson and J. V. Smith, *J. Am. Chem. Soc.*, 1987, **109**, 3639-3646; (c) Z. Zongyan, L. Zhaosheng and Z. Zhigang, *J Phys: Condens Matter*, 2010, **22**, 175008.

30 (a) R. Erdogan, O. Ozbek and I. Onal, *Surf. Sci.*, 2010, **604**, 1029-1033; (b) J. Guo, S. Watanabe, M. J. Janik, X. Ma and C. Song, *Catal. Today*, 2010, **149**, 218-223; (c) A. Hussain, J. Gracia, B. E. Nieuwenhuys and J. W. Niemantsverdriet, *Chemphyschem*, 2010, **11**, 2375-2382.

31 A. Vittadini and M. Casarin, *Theor. Chem. Acc.*, 2008, **120**, 551-556.

32 (a) X.-Q. Gong and A. Selloni, *J. Phys. Chem. B*, 2005, **109**, 19560-19562; (b)

V. M. Bermudez, *J. Phys. Chem. C,* 2011, **115**, 6741-6747.

33 J. D. Gale and A. L. Rohl, *Mol. Simulat.*, 2003, **29**, 291-341.

34 K. Hameeuw, G. Cantele, D. Ninno, F. Trani and G. Iadonisi, *J. Chem. Phys.*, 2006, **124**, 024708.

35 H. Liu, X. Wang, C. Pan and K. M. Liew, *J. Phys. Chem. C*, 2012, **116**, 8044-8053.

36 I. G. Austin and N. F. Mott, *Adv. Phys.*, 2001, **50**, 757-812.

37 S. Wendt, P. T. Sprunger, E. Lira, G. K. H. Madsen, Z. Li, J. Ø. Hansen, J. Matthiesen, A. Blekinge-Rasmussen, E. Lægsgaard, B. Hammer and F. Besenbacher, *Science*, 2008, **320**, 1755-1759.

38 (a) M. Che and A. J. Tench, in *Adv. Catal.*, eds. H. P. D.D. Eley and B. W. Paul, Academic Press1983, vol. Volume 32, pp. 1-148; (b) M. Anpo, M. Che, B. Fubini, E. Garrone, E. Giamello and M. Paganini, *Top. Catal.*, 1999, **8**, 189-198.

39 G. Pacchioni, A. M. Ferrari and E. Giamello, *Chem. Phys. Lett.*, 1996, **255**, 58-64.

40 A. Fujishima, X. Zhang and D. A. Tryk, *Surf. Sci. Rep.*, 2008, **63**, 515-582.

41 C. Di Valentin, G. Pacchioni and A. Selloni, *J. Phys. Chem. C*, 2009, **113**, 20543 - 20552.

42 (a) M. Casarin, C. Maccato and A. Vittadini, *J. Phys. Chem. B*, 2002, **106**, 795-802; (b) M. Casarin, M. Nardi and A. Vittadini, *Surf. Sci.*, 2004, **566**, 451-456; (c) A. J. Lupinetti, S. Fau, G. Frenking and S. H. Strauss, *J. Phys. Chem. A*, 1997, **101**, 9551-9559; (d) M. Casarin and A. Vittadini, *Surf. Sci.*, 1997, **387**, L1079-L1084; (e)

M. Casarin, C. Maccato and A. Vittadini, *Chem. Phys. Lett.*, 1997, **280**, 53-58.

43 (a) Y. Iizuka, H. Fujiki, N. Yamauchi, T. Chijiiwa, S. Arai, S. Tsubota and M. Haruta, *Catal. Today*, 1997, **36**, 115-123; (b) P. K. Dutta, A. Ginwalla, B. Hogg, B. R. Patton, B. Chwieroth, Z. Liang, P. Gouma, M. Mills and S. Akbar, *J. Phys. Chem. B*, 1999, **103**, 4412-4422; (c) G. Martra, *Appl. Catal., A*, 2000, **200**, 275-285.

44 J. Scaranto and S. Giorgianni, *Mol. Phys.*, 2009, **107**, 1997-2003.

45 X. H. Yang, Z. Li, C. Sun, H. G. Yang and C. Li, *Chem. Mater.*, 2011, **23**, 3486-3494.

46 A. Rohrbach, J. Hafner and G. Kresse, *Phys. Rev. B*, 2004, **69**, 075413.

47 A. Rohrbach and J. Hafner, *Phys. Rev. B*, 2005, **71**, 045405.

48 Z. Liu, L. Ma and A. S. M. Junaid, *J. Phys. Chem. C,* 2010, **114**, 4445-4450.

49 (a) A. V. Slack and G. A. Hollinden, 1975; (b) J. A. Rodriguez, G. Liu, T. Jirsak, J. Hrbek, Z. Chang, J. Dvorak and A. Maiti, *J. Am. Chem. Soc.*, 2002, **124**, 5242-5250.

50 A. PiÉPlu, O. Saur, J.-C. Lavalley, O. Legendre and C. NÉDez, *Catal. Rev.*, 1998, **40**, 409-450.

51 (a) K. E. Smith, J. L. Mackay and V. E. Henrich, *Phys. Rev. B*, 1987, **35**, 5822-5829; (b) H. Onishi, T. Aruga, C. Egawa and Y. Iwasawa, *Surf. Sci.*, 1988, **193**, 33-46; (c) E. Román, J. L. de Segovia, J. A. Martín-Gago, G. Comtet and L. Hellner, *Vacuum*, 1997, **48**, 597-600; (d) D. I. Sayago, P. Serrano, O. Böhme, A. Goldoni, G. Paolucci, E. Román and J. A. Martín-Gago, *Phys. Rev. B*, 2001, **64**, 205402.

52 (a) M. Casarin, F. Ferrigato, C. Maccato and A. Vittadini, *J. Phys. Chem. B*,

2005, **109**, 12596-12602; (b) C. Zhang and P. J. Lindan, *Chem. Phys. Lett.*, 2003, **373**, 15-21; (c) R. De Francesco, M. Stener and G. Fronzoni, *Phys. Chem. Chem. Phys.*, 2009, **11**, 1146-1151.

53 S. Chaturvedi, J. A. Rodriguez, T. Jirsak and J. Hrbek, *J. Phys. Chem. B*, 1998, **102**, 7033-7043.

54 (a) J. Haase, *J. Phys: Condens. Matter.*, 1997, **9**, 3647; (b) D. M. P. Mingos, *Transit. Metal Chem.*, 1978, **3**, 1-15.

55 N. Pangher, L. Wilde, M. Polcik and J. Haase, *Surf. Sci.*, 1997, **372**, 211-222.

56 (a) S. Mehandru and A. B. Anderson, *J. Electrochem. Soc.*, 1986, **133**, 828-832; (b) X. Lin, K. C. Hass, W. F. Schneider and B. L. Trout, *J. Phys. Chem. B*, 2002, **106**, 12575-12583; (c) R. Jiang, W. Guo, M. Li, H. Zhu, J. Li, L. Zhao, D. Fu and H. Shan, *J. Phys. Chem. C,* 2009, **113**, 18223-18232.

57 (a) M. L. Burke and R. J. Madix, *Surf. Sci.*, 1988, **194**, 223-244; (b) S. Terada, T. Yokoyama, M. Sakano, M. Kiguchi, Y. Kitajima and T. Ohta, *Chem. Phys. Lett.*, 1999, **300**, 645-650; (c) G. J. Jackson, S. M. Driver, D. P. Woodruff, N. Abrams, R. G. Jones, M. T. Butterfield, M. D. Crapper, B. C. C. Cowie and V. Formoso, *Surf. Sci.*, 2000, **459**, 231-244.

TOC: